Attention-Deficit/Hyperactivity Disorder Symptoms Coincide With Altered Striatal Connectivity

Supplemental Information

Contents

Instantaneous Correlation Parcellation of Striatum

To segment the striatum into functional subregions, we used a novel top-down parcellation strategy called Instantaneous Correlation Parcellation (ICP; Van Oort *et al.*, in preparation). ICP is based on the assumption that voxels that form a subregion within a larger region of interest (ROI) exhibit similar, yet slightly different time courses compared to other voxels within the larger region. Accordingly, each subregion within this ROI could be identified by structured changes between the voxel-wise timeseries and thus has its own characteristic temporal signature. To enhance the identifiability of subregions, ICP selectively augments these subtle differences by the element-wise multiplication of the voxel-wise time courses with the average time course of the entire ROI. This process (called "temporal unfolding") results in instantaneous correlations and is illustrated in Figure S1. The instantaneous correlations are calculated separately for every fMRI dataset. Subsequently, group-level independent component analysis (ICA; 1), a data-driven multivariate analyses technique, is applied to these transformed time courses. ICA will divide the ROI into subregions (i.e., components) by grouping voxels with similar timeseries, thus segregating voxels with different instantaneous correlations.

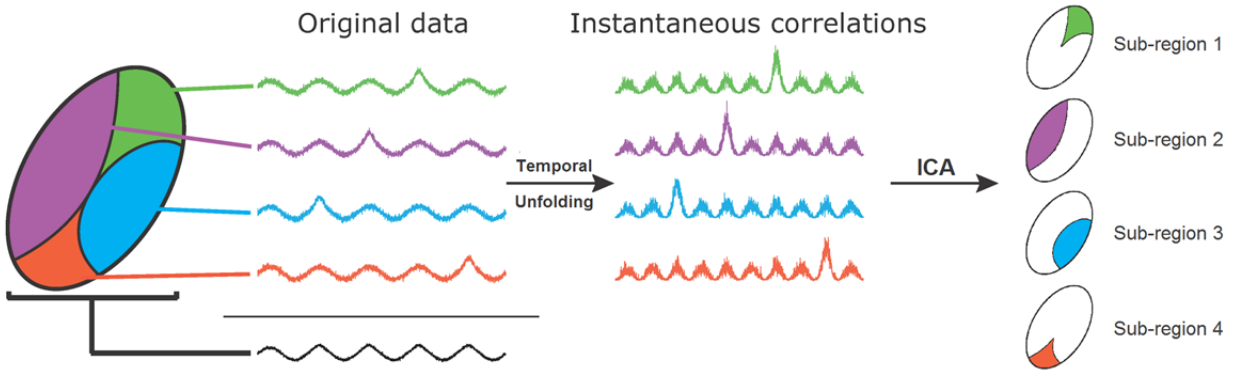

Figure S1. Illustration of the instantaneous correlation parcellation strategy. The oval represents a ROI consisting of four subregions. The black time course represents the average timeseries of the entire ROI, whereas the four colored timeseries represent exemplar timeseries for a voxel within each subregion. Multiplying each of these voxel specific timeseries with the average time course of the entire ROI (temporal unfolding), results in instantaneous correlations in which the subtle differences between the timeseries of each voxel are enhanced (increase in SNR of about 3 dB in this example). Subsequently, ICA is applied to the unfolded timeseries to segregate the region of interest into subregions by grouping voxels with similar instantaneous correlations.

To determine which number of subregions is best supported by the data, or in other words, in how many subregions a ROI can be functionally segregated, ICP employs split-half reproducibility analyses for a selected range of model orders (i.e., the number of subregions, also referred to as the

scale of parcellation). To this end the group ICA is repeated in two random halves of the rs-fMRI datasets for every scale. Subsequently, the split-half reproducibility at each scale is determined by calculating the Dice-overlap between the obtained parcellations for each half of the datasets. By iterating this process 20 times, reliable averages are acquired for each scale and the optimal scale of parcellation can be defined. Figure S2 illustrates the ICP pipeline.

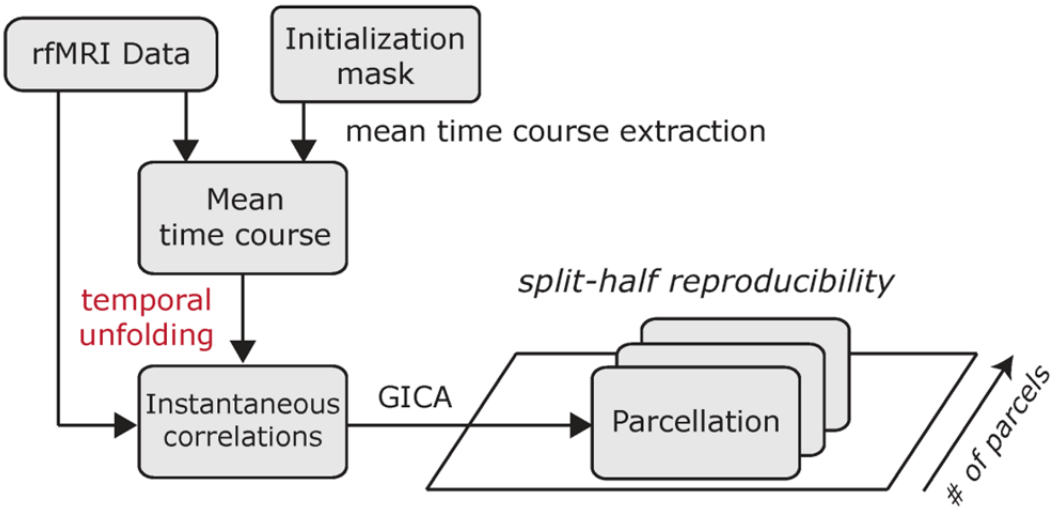

Figure S2. Flowchart of the ICP pipeline. The group ICA is applied to the instantaneous correlations and repeated 20 times for a range of model orders in order to assess split-half reproducibility.

Here, we applied ICP to obtain parcellations of striatum ranging from two to 30 subregions using rs-fMRI data of 100 participants from the HCP dataset. Specifically, we selected the first 50 females and first 50 males belonging to the 26-30 age range from the S500 release (see Table S1 for the subjects IDs). As a first solution, ICP yielded highest split-half reproducibility for a parcellation including two subregions (Figure S3). This parcellation segregated the striatum into a region corresponding to putamen and a region corresponding to NAcc and caudate. However, since we were interested in a small-scale subdivision of striatum, we selected the parcellation of striatum into six subregions. This parcellation had the second highest reproducibility with an average Dice-overlap of 84% between repeat analyses (see Figure S3). To further enhance the stability of the obtained subregions we identified those voxels within each subregion that were part of the same subregion across the lower-scale parcellations. This resulted in coherent, stable subregions that we used as seeds in subsequent functional connectivity analyses. This stable parcellation and the parcellations up to six clusters are depicted in Figure S4.

Table S1. Subjects IDs from HCP subjects included in the ICP analysis.

Subject IDs							
101309	123925	148941	169444	187143	209834	385450	833148
102311	128127	149741	171431	189349	210415	395958	837560
103111	131217	150625	171633	191033	211215	433839	871762
105014	131722	152831	172029	191336	211922	445543	901038
106521	132118	154936	172130	191841	212116	573249	910241
108121	133019	155635	173334	192843	212419	594156	912447
108323	135528	157437	173435	194645	231928	599671	922854
111413	140117	159441	173940	197348	290136	623844	958976
116524	141826	160830	177645	198855	303119	690152	983773
118528	142626	161630	178142	201818	308331	695768	
120515	145834	164131	179346	203418	316633	742549	
122620	146331	164939	180129	205220	352132	789373	
123420	147030	167036	181232	208327	380036	814649	

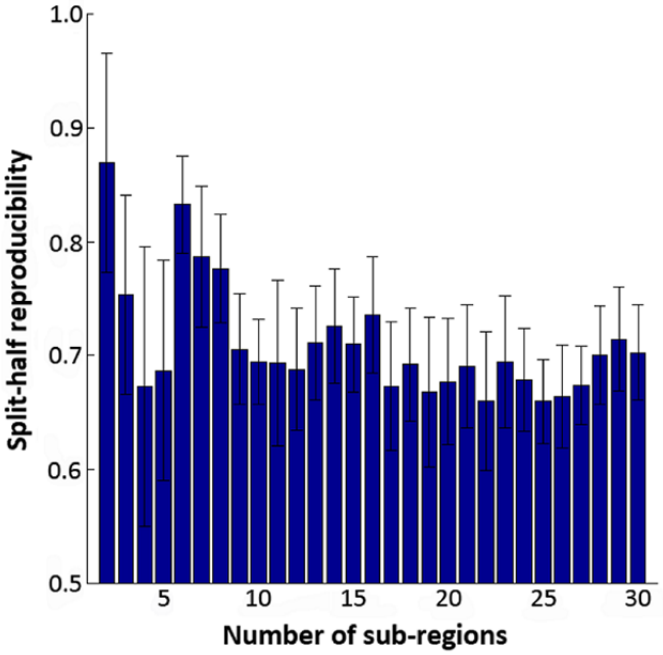

Figure S3. The split-half reproducibility score at each scale of the functional parcellations obtained for the striatum in the HCP sample.

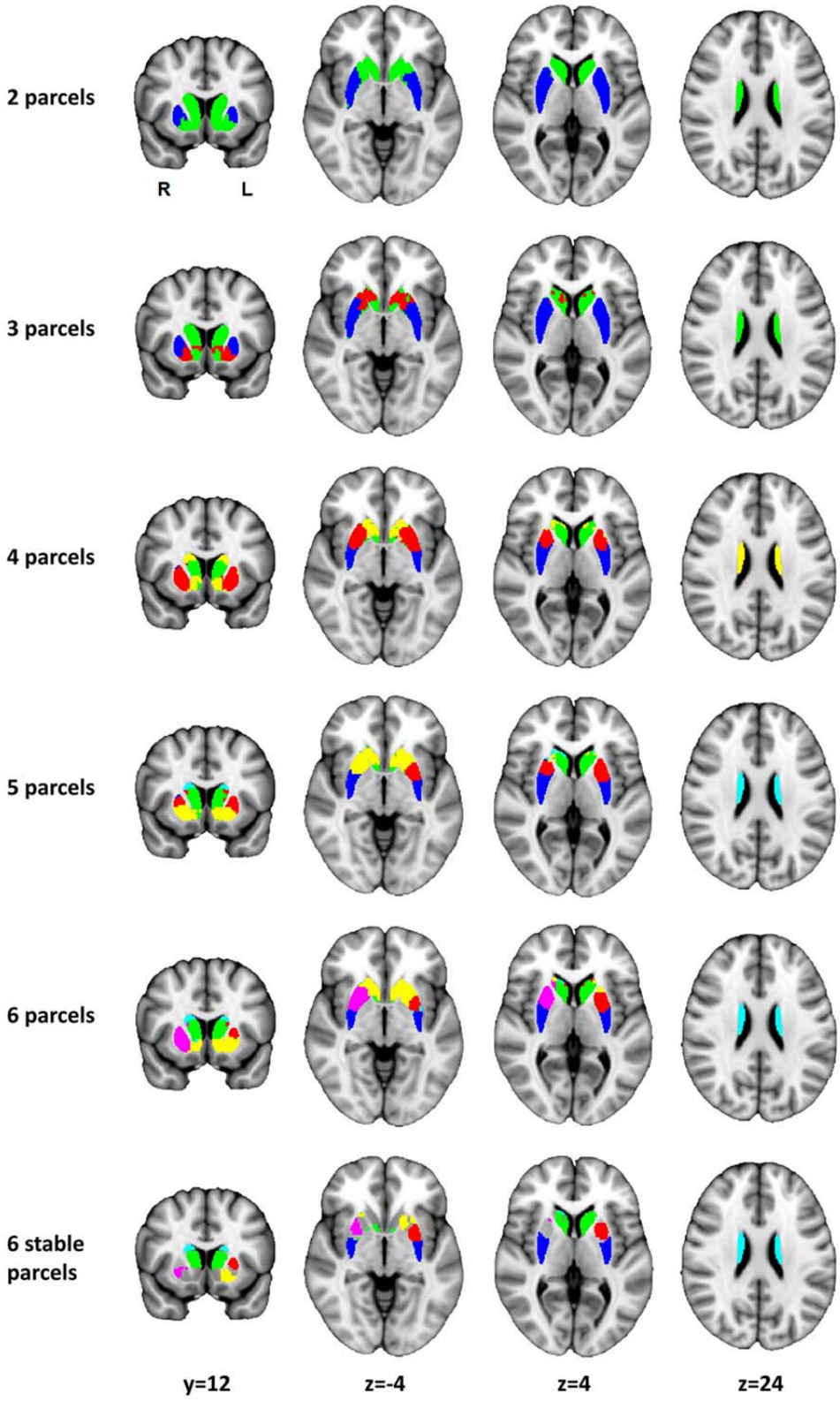

Figure S4. Functional parcellations of the striatum ranging from two to six subregions and the six stable subregions that were used as seed regions in further analyses.

Discussion of Striatal Parcellation and Cortico-striatal Networks in Light of Previous Literature

A functional parcellation of the striatum has been generated before (2-4). Choi and colleagues (2) used seven cortical networks obtained by (5) and assigned each voxel in the striatum to its most strongly correlated cortical network, resulting in a striatal parcellation consisting of seven subregions. Figure S5 shows a comparison between this parcellation and our ICP parcellation of the striatum. Some overlap between both parcellations is present, for example both parcellations contain subregions for anterior putamen and consist of a more dorsal and a more ventral part of the caudate. Nevertheless, the parcellations are clearly distinct. Although this might partly relate to the difference in the number of subregions (i.e., seven versus six subregions), it is more likely related to differences in methodology. Whereas the parcellation of Choi and colleagues is based on connectivity with cortex, our parcellation is solely based on the internal signal homogeneity of striatum.

Similar to our study, Di Martino and colleagues (6) also investigated functional connectivity of the striatum using a seed-based approach. Yet, instead of parcellating striatum into subregions and determining functional connectivity of these subregions in a multivariate analysis, they placed six spherical seed regions (with a radius of 3.5 mm, including 123 isotropic 1 mm voxels) in the striatum and computed functional connectivity for each seed in a separate analysis. A comparison of the six seed-regions as well as the obtained functional networks between both studies is displayed in Figure S6. The seed regions from the study of Di Martino and colleagues are smaller compared to our seed regions (Figure S6A). The ventral caudate region defined by our parcellation includes both the dorsal caudate and ventral striatum superior defined in the Di Martino study, whereas the NAcc region defined in our parcellation includes the ventral striatum inferior region defined in the Di Martino study. Our anterior putamen regions include the ventral rostral putamen and our posterior putamen region includes the dorsal caudal putamen regions defined in the study of Di Martino. However, our parcellation does not include a dorsal rostral putamen region. Furthermore, it is important to note that the networks displayed for the Di Martino study (panel B) are based on the right striatal seeds only, whereas our seed regions were unilateral or bilateral depending on the subregion (panel C). Comparing the functional networks between studies reveals similarities but also differences. For example, the posterior putamen network defined in our study is much more extended than the network of the corresponding dorsal caudal putamen region defined in the study of Di Martino, but both networks include the primary motor cortex. Furthermore, the network of the ventral caudate region defined in our study, shows great overlap with the network of the ventral striatum superior and the dorsal caudate seed region obtained in the Di Martino study. However, the networks of the NAcc and anterior putamen show more

differences than similarities with the corresponding networks in the study of Di Martino and colleagues. Differences in location and size of the seed regions as well as distinct methodology, i.e., univariate versus multivariate analyses, likely contribute to differences in functional networks between both studies.

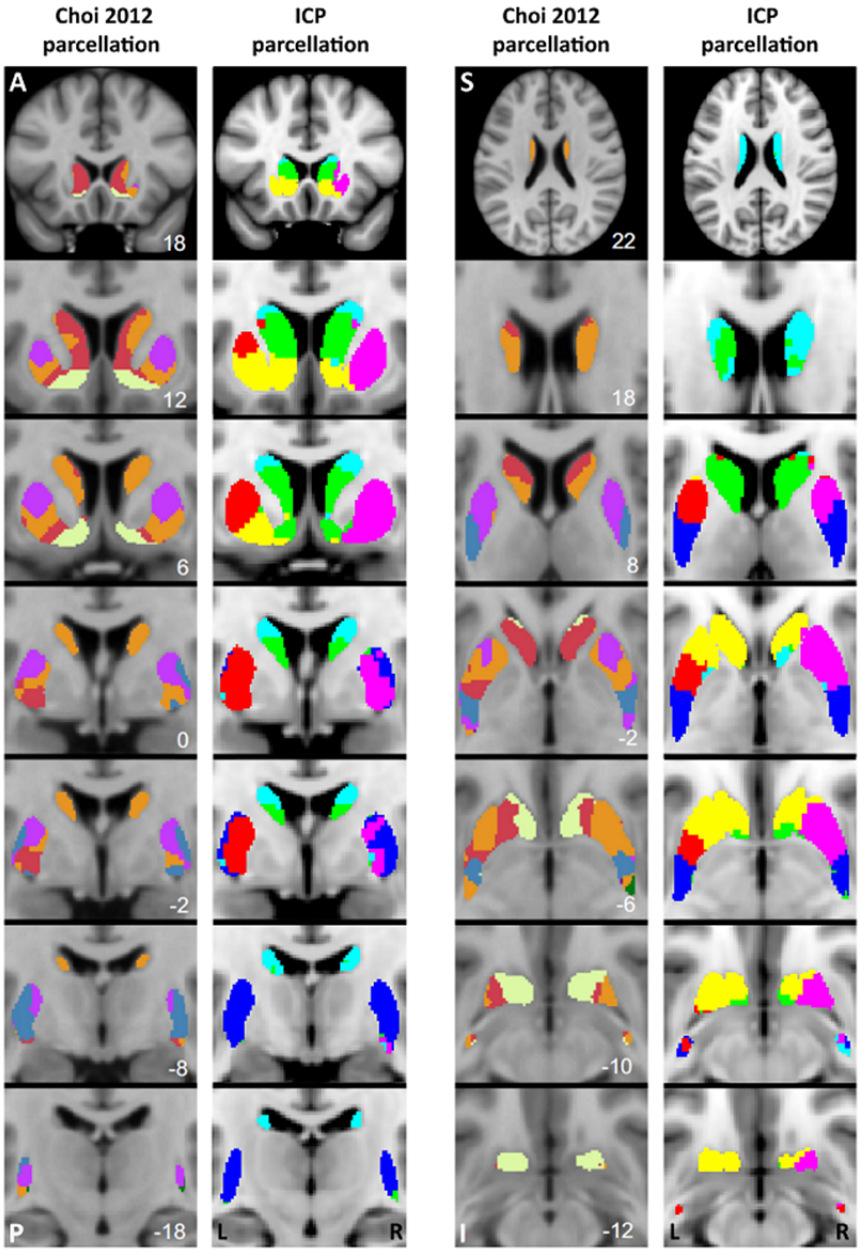

Figure S5. Comparison between the functional parcellation of the striatum into seven subregions described in (2; figure modified with permission) and our ICP parcellation into six subregions. Slices from anterior to posterior in the brain are shown on the left, slices from superior to inferior on the right. Numbers indicate Y-coordinates (left) and Z-coordinates (right) in MNI space. A, anterior; I, inferior; L, left; P, posterior; R, right; S, superior.

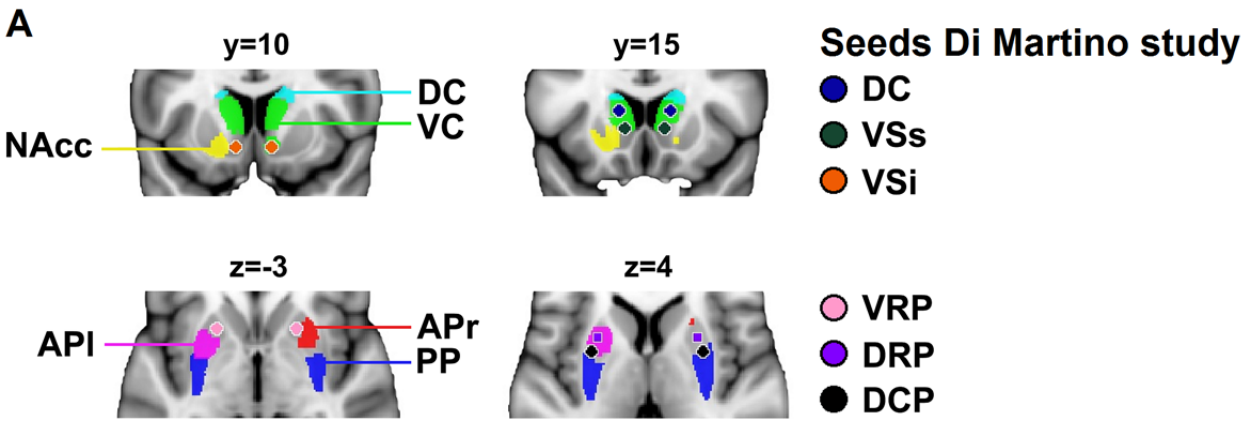

Figure S6A. Comparison between the six striatal seed regions used in our study and the six spherical seeds used in the study of Di Martino and colleagues (6). The six spherical seeds of the Di Martino study are placed on top of our ICP-defined seed regions. APl, left anterior putamen; APr, right anterior putamen; DC, dorsal caudate; DCP, dorsal caudal putamen; DRP, dorsal rostral putamen; NAcc, nucleus accumbens; PP, posterior putamen; VC, ventral caudate; VRP, ventral rostral putamen; VSi, ventral striatum inferior; VSs, ventral striatum superior.

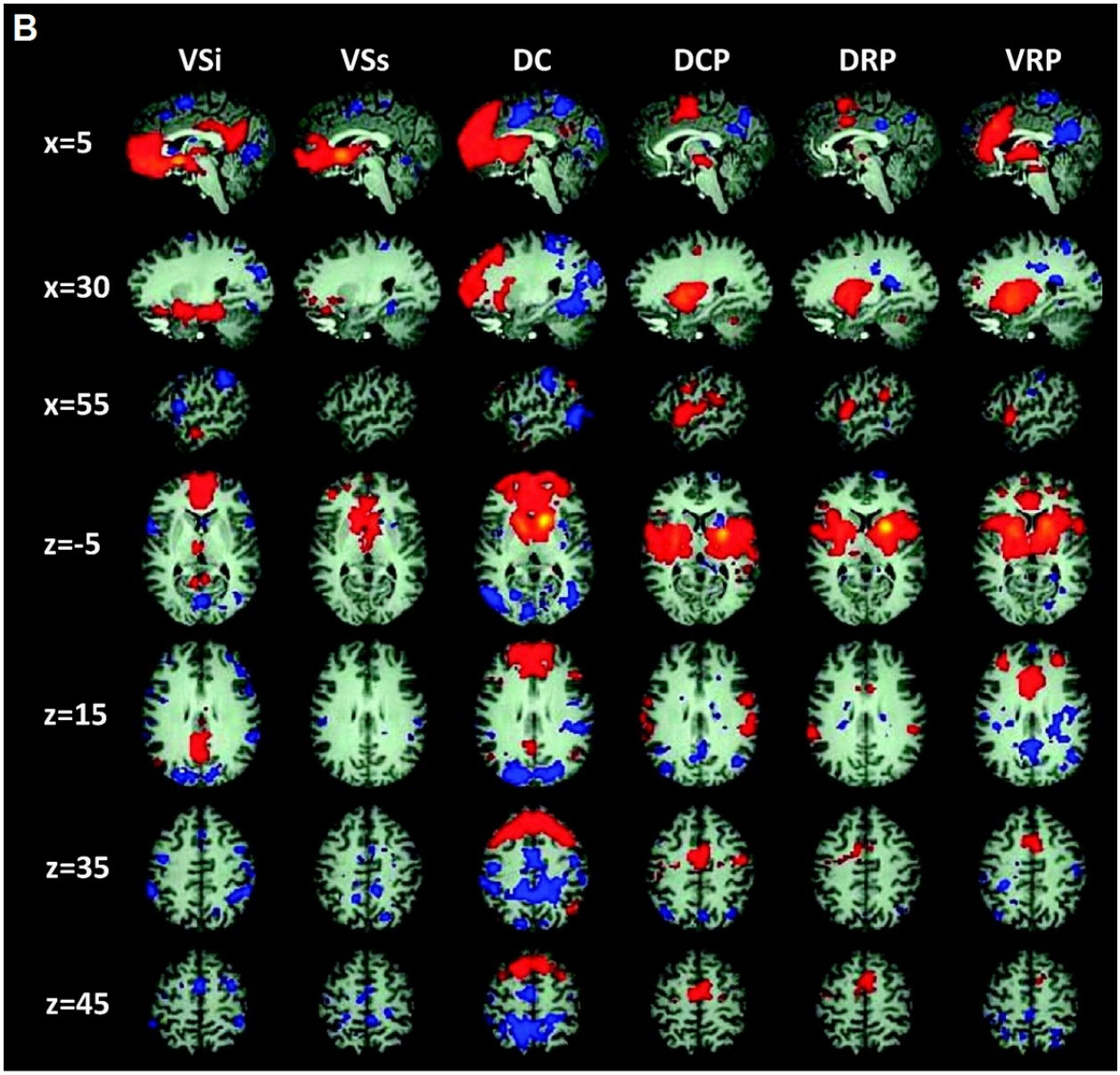

Figure S6B. The six functional networks described by Di Martino and colleagues (6), *Z* score > 3.1, cluster significance: $p < .01$, corrected. X-values and z-values represent x and z MNI-coordinates respectively. DC, dorsal caudate; DCP, dorsal caudal putamen; DRP, dorsal rostral putamen; VRP, ventral rostral putamen; VSi, ventral striatum inferior; VSs, ventral striatum superior.

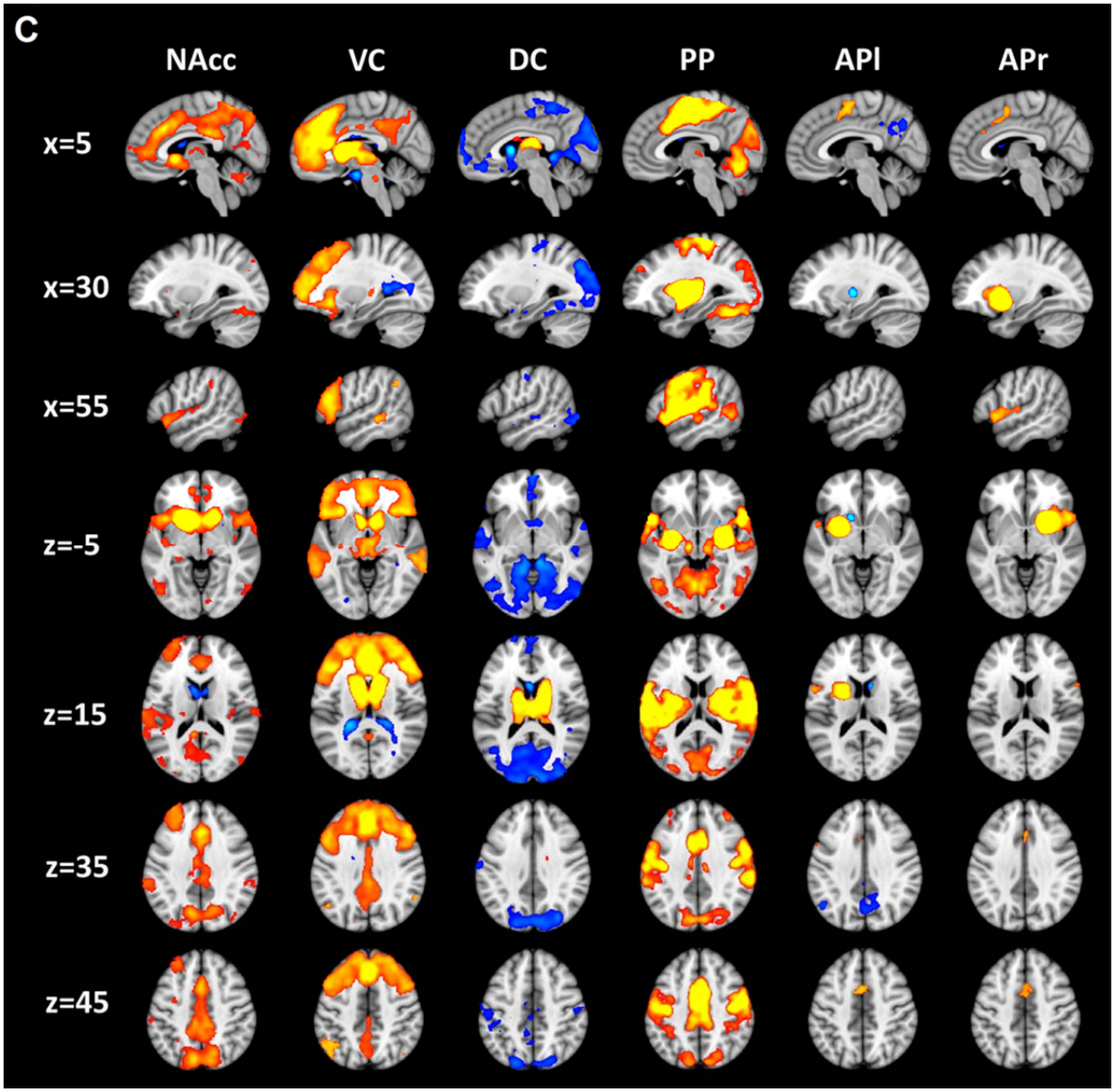

Figure S6C. The six functional networks obtained in our study, *T* score > 4.0, cluster significance: $p < .0083$, corrected. APl, left anterior putamen; APr, right anterior putamen; DC, dorsal caudate; NAcc, nucleus accumbens; PP, posterior putamen; VC, ventral caudate.

MRI Data Acquisition and Preprocessing

MRI data were acquired at two locations on 1.5 Tesla Siemens scanners from Siemens (Siemens AVANTO at the Donders Institute for Brain Cognition and Behavior in Nijmegen and Siemens SONATA at the VU University Medical Centre in Amsterdam). At both sites identical 8-channel head coils and MRI protocols were employed. An MPRAGE sequence was used for the acquisition of T1-weighted anatomical scans (TR = 2730 ms, TE = 2.95 ms, TI = 1000 ms, voxel size = 1 x 1 x 1 mm, flip angle = 7˚, matrix size = 256 x 256, FOV = 256 mm, 176 slices). The rs-fMRI data were obtained using a gradient echo-planar imaging (GE-EPI) sequence (TR = 1960 ms, TE = 40 ms, flip angle = 80, matrix size = 64 x 64, in-plane resolution = 3.5 mm, FOV = 224 mm, 37 axial slices, slice thickness/gap = 3.0 mm/0.5 mm, 265 volumes). Participants were instructed to relax and keep their eyes open for the duration of the rs-fMRI scan.

Tools from the FMRIB Software Library (FSL version 5.0.6; http://www.fmrib.ox.ac.uk/fsl) were used for preprocessing of the rs-fMRI data. We applied a standard preprocessing pipeline which included removal of the first five volumes allowing for signal equilibration, primary head movement correction via realignment to the middle volume (MCFLIRT; 7), grand mean scaling, and spatial smoothing using a 6 mm FWHM Gaussian kernel. We did not conduct band-pass filtering in an effort to preserve as much signal of interest as possible. Moreover, in light of frequency aliasing given our volume TR we believe that respiration or cardiac-related signal would not be adequately removed using the typical 0.1–0.01 Hz band-pass filter. The preprocessed rs-fMRI data were denoised for secondary head motion-related artifacts using automatic noise selection as implemented in ICA-AROMA (8), a novel method for distinguishing head motion-related components resulting from an ICA decomposition of the preprocessed data. Importantly the selection of components made by ICA-AROMA preserves reproducibility and identifiability of resting-state signal of interest (9). Finally, signal from white matter and cerebrospinal fluid was removed using nuisance regression, and a high-pass filter (0.01 Hz) was applied. Each participants' rs-fMRI images were coregistered to the participants' anatomical image using boundary-based registration implemented in FSL-FLIRT (10). The T1 images were registered to Montreal Neurological Institute (MNI152) standard space using 12-parameter affine transformation and refined using non-linear registration with FSL-FNIRT (10 mm warp, 2 mm resampling resolution; 7).

Scatterplots of the Observed Dimensional ADHD-Related Effects

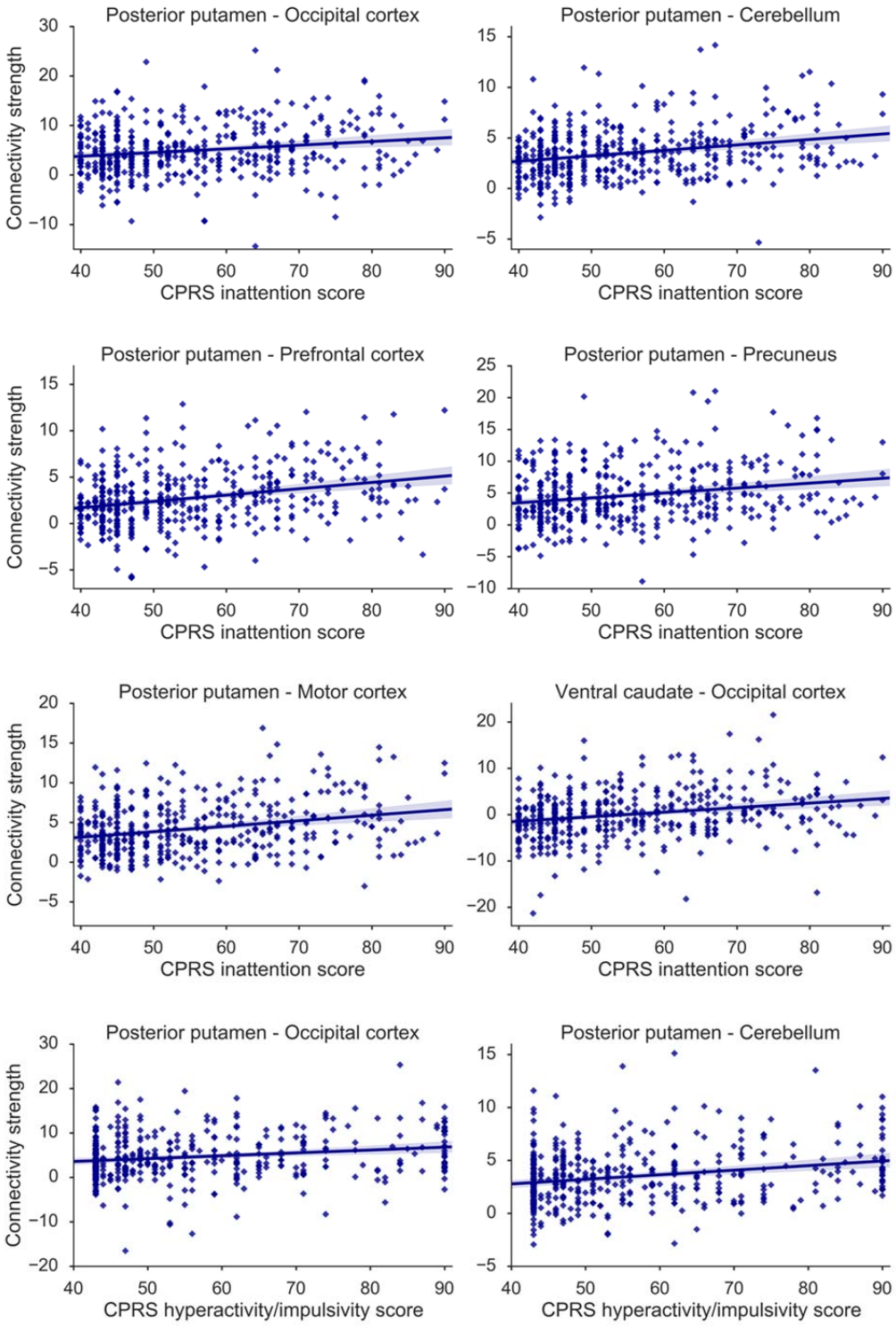

Figure S7. Representation of the observed dimensional relationships between Conners Parent Rating Scale (CPRS) inattention and CPRS hyperactivity/impulsivity scores and functional connectivity of posterior putamen and ventral caudate across all participants.

Post-hoc Sensitivity Analyses of the Observed Dimensional ADHD-Related Effects

We conducted post-hoc sensitivity analyses to ensure that our observed symptom related increases in functional connectivity in the networks of posterior putamen and ventral caudate were not driven by effects of age, IQ, and medication use. To this end we computed correlations between age, IQ, and duration of medication use (days; only in the ADHD group), and functional connectivity of posterior putamen with clusters that showed a significant inattention-related increase in occipital cortex, cerebellum, precuneus, motor cortex, and prefrontal cortex (i.e., the mean value for each cluster; corrected for age, sex, scan location, and oppositional defiant disorder (ODD)/conduct disorder (CD) comorbidity). Similarly, we computed correlations between age, IQ, and duration of medication use, and functional connectivity of posterior putamen with clusters in occipital cortex and cerebellum that showed a significant hyperactivity/impulsivity-related increase. Table S2 demonstrates that none of these correlations survived correction for multiple comparisons, confirming that age, IQ, and medication use did not influence the observed symptom-related increases in functional connectivity. We note the trend in the correlations with medication duration in the ADHD sample; these could provide interesting angles for further investigation.

To ensure that the observed symptom-related increases in functional connectivity in the networks of posterior putamen and ventral caudate were not specific to sex, scan location, and presence or absence of ODD/CD comorbidity, we furthermore computed correlations between Conners Parent Rating Scale (CPRS) inattention scores and CPRS hyperactivity/impulsivity scores (11) and functional connectivity of posterior putamen and ventral caudate with their significant clusters (i.e., the mean value for each cluster) separately for males and for females, for participants scanned in Amsterdam and in Nijmegen, and for participants without and with ODD/CD comorbidity. These analyses aimed to qualitatively confirm that effects within each subgroup adhere to the same direction as our main findings (i.e., symptom related increases in functional connectivity), rather than demonstrating that effects within subgroups remained significant, as splitting into smaller groups will affect statistical power. These analyses demonstrated inattention-related increases in functional connectivity of posterior putamen and ventral caudate and hyperactivity/impulsivity-related increases in functional connectivity of posterior putamen, in males as well as in females, for participants scanned in Amsterdam and in Nijmegen, and for participants without as well as with ODD/CD comorbidity (Table S3). Apart from the correlations between ventral caudate-occipital cortex connectivity and inattentive symptoms and between posterior putamen-occipital cortex connectivity and hyperactive/impulsive symptoms in the ODD/CD comorbidity group, all correlations were positive, and comparable between

those obtained for males and females, Nijmegen and Amsterdam and with or without ODD/CD comorbidity. These analyses confirm that the observed inattention and hyperactivity-related increases in functional connectivity in the networks of posterior putamen and ventral caudate were not driven by differences in sex, scan location, and ODD/CD comorbidity.

Table S2. Correlations and corresponding *p*-values of posterior putamen-occipital cortex, posterior putamen-cerebellum, posterior putamen-precuneus, posterior putamen-motor cortex, posterior putamen-prefrontal cortex, and ventral caudate-occipital cortex functional connectivity with age, (estimated) IQ, and duration of medication use (in the ADHD group).

Functional Connectivity ***Inattention-Related Increase***		**Age**	**IQ**	**Medication Duration**
Posterior putamen – Occipital cortex	*r* =	-0.05	0.05	-0.17
	p =	0.32	0.34	0.05
Posterior putamen – Cerebellum	*r* =	-0.07	-0.01	0.003
	p =	0.15	0.88	0.98
Posterior putamen – Precuneus	*r* =	-0.03	0.03	-0.17
	p =	0.50	0.60	0.04
Posterior putamen – Motor cortex	*r* =	-0.06	0.01	-0.12
	p =	0.21	0.87	0.16
Posterior putamen – Prefrontal cortex	*r* =	0.02	0.02	-0.16
	p =	0.65	0.66	0.06
Ventral caudate – Occipital cortex	*r* =	-0.03	0.03	0.01
	p =	0.50	0.59	0.86
Functional Connectivity ***Hyperactivity/Impulsivity-Related Increase***				
Posterior putamen – Occipital cortex	*r* =	-0.04	0.04	-0.16
	p =	0.36	0.42	0.05
Posterior putamen – Cerebellum	*r* =	-0.05	-0.02	-0.03
	p =	0.25	0.66	0.70

Table S3. Correlations and corresponding *p*-values between Conners Parent Rating Scale (CPRS) inattention scores and posterior putamen-occipital cortex, posterior putamen-cerebellum, posterior putamen-precuneus, posterior putamen-motor cortex, posterior putamen-prefrontal cortex, and ventral caudate-occipital cortex functional connectivity, and between CPRS hyperactivity/impulsivity scores and posterior putamen-occipital cortex and posterior putamen-cerebellum functional connectivity, calculated separately for males and females, for participants scanned in Nijmegen and Amsterdam, and for participants without and with oppositional defiant disorder (ODD)/conduct disorder (CD) comorbidity. Corrected for effects of age, sex, scan location, and ODD/CD comorbidity. *$p < 0.05$, **$p < 0.001$.

		Sex		**Scan Location**		**ODD/CD Comorbidity**	
Inattention-Related Increase		Male *n* = 250	Female *n* = 194	Nijmegen *n* = 222	Amsterdam *n* = 222	No ODD/CD *n* = 387	ODD/CD *n* = 57
Posterior putamen – Occipital cortex	*r* =	0.24	0.20	0.30	0.12	0.22	0.13
	p =	**	*	**	0.09	**	0.37
Posterior putamen – Cerebellum	*r* =	0.33	0.24	0.39	0.18	0.29	0.28
	p =	**	*	**	*	**	*
Posterior putamen – Precuneus	*r* =	0.25	0.23	0.27	0.21	0.25	0.18
	p =	**	*	**	*	**	0.19
Posterior putamen – Motor cortex	*r* =	0.28	0.30	0.30	0.27	0.30	0.25
	p =	**	**	**	**	**	0.07
Posterior putamen – Prefrontal cortex	*r* =	0.37	0.17	0.29	0.27	0.29	0.28
	p =	**	*	**	**	**	*
Ventral caudate – Occipital cortex	*r* =	0.23	0.31	0.25	0.27	0.30	0.06
	p =	**	**	**	**	**	0.66
Hyperactivity/ Impulsivity-Related Increase							
Posterior putamen – Occipital cortex	*r* =	0.19	0.26	0.26	0.18	0.26	0.00
	p =	*	**	**	*	**	0.96
Posterior putamen – Cerebellum	*r* =	0.29	0.22	0.34	0.18	0.26	0.30
	p =	**	*	**	*	**	*

In addition, we computed correlations between CPRS inattention scores and CPRS hyperactivity/impulsivity scores and functional connectivity of posterior putamen and ventral caudate with their significant clusters in each of the four diagnostic groups separately (i.e., controls, ADHD, unaffected siblings, and subthreshold ADHD; Table S4). These analyses aimed to show that effects in each of these groups adhere to the same direction as our main findings (i.e., symptom related increases in functional connectivity), rather than demonstrating that correlations within subgroups remained significant, as splitting into smaller groups will affect statistical power. As can be observed in Table S4, the relationship of functional connectivity with inattention and hyperactivity/impulsivity scores was strongest in ADHD participants and their unaffected siblings. Overall, correlations between functional connectivity and symptom scores were also positive in the control group, but they were weaker,

possibly as a result of the smaller range of symptom scores covered by the control group compared to the other diagnostic groups.

Table S4. Correlations between Conners Parent Rating Scale (CPRS) inattention scores and posterior putamen-occipital cortex, posterior putamen-cerebellum, posterior putamen-precuneus, posterior putamen-motor cortex, posterior putamen-prefrontal cortex, and ventral caudate-occipital cortex functional connectivity, and between CPRS hyperactivity/impulsivity scores and posterior putamen-occipital cortex and posterior putamen-cerebellum functional connectivity, calculated separately in each diagnostic group. Corrected for effects of age, sex, scan location, and opposition defiant disorder/conduct disorder comorbidity.

Functional Connectivity ***Inattention-Related Increase***		**All** (*n* = 444)	**Control** (*n* = 122)	**ADHD** (*n* = 169)	**Sibling** (*n* = 89)	**Subthreshold** (*n* = 64)
Posterior putamen – Occipital cortex	*r* =	0.22	-0.04	0.11	0.25	0.12
Posterior putamen – Cerebellum	*r* =	0.29	0.13	0.17	0.33	0.004
Posterior putamen – Precuneus	*r* =	0.28	0.03	0.27	0.35	-0.08
Posterior putamen – Motor cortex	*r* =	0.28	0.02	0.24	0.13	-0.02
Posterior putamen – Prefrontal cortex	*r* =	0.24	0.04	0.17	0.14	-0.02
Ventral caudate – Occipital cortex	*r* =	0.26	0.26	0.18	0.22	0.06
Functional Connectivity ***Hyperactivity/Impulsivity-Related Increase***						
Posterior putamen – Occipital cortex	*r* =	0.22	0.19	0.12	0.08	0.02
Posterior putamen – Cerebellum	*r* =	0.26	0.03	0.14	0.26	0.04

Further, we investigated whether medication status within the ADHD group influenced our findings. To this end, we computed correlations between CPRS inattention scores and CPRS hyperactivity/impulsivity scores and functional connectivity of posterior putamen and ventral caudate with their significant clusters separately in medicated and medication-naïve ADHD participants (see Table S5 and Figure S8). These analyses aimed to show that effects in both groups adhere to the same direction as our main findings (i.e., symptom related increases in functional connectivity), rather than demonstrating that correlations within subgroups remained significant, as splitting into smaller groups will affect statistical power. As can be observed in Table S5 and Figure S8, the relationship between ADHD symptom scores appears similar in medicated and medication-naïve ADHD subjects, indicating that medication status only minimally influenced our findings. Moreover, when assessing the scatter

plots presented in Figure S8 it is clear that the medicated and medication-naïve participants are indistinguishable from each other, adding to the conclusion that in our analyses there was no effect of medication status.

Table S5. Correlations between Conners Parent Rating Scale (CPRS) inattention scores and posterior putamen-occipital cortex, posterior putamen-cerebellum, posterior putamen-precuneus, posterior putamen-motor cortex, posterior putamen-prefrontal cortex, and ventral caudate-occipital cortex functional connectivity, and between CPRS hyperactivity/impulsivity scores and posterior putamen-occipital cortex and posterior putamen-cerebellum functional connectivity, calculated separately in for the medicated and medication-naïve ADHD participants. Corrected for effects of age, sex, scan location, and oppositional defiant disorder/conduct disorder comorbidity.

Functional Connectivity ***Inattention-Related Increase***		**All ADHD** (*n* = 169)	**ADHD Medicated** (*n* = 130)	**ADHD Medication-Naïve** (*n* = 39)
Posterior putamen – Occipital cortex	*r* =	0.11	0.17	0.31
Posterior putamen – Cerebellum	*r* =	0.17	0.23	0.24
Posterior putamen – Precuneus	*r* =	0.27	0.25	0.24
Posterior putamen – Motor cortex	*r* =	0.24	0.38	0.20
Posterior putamen – Prefrontal cortex	*r* =	0.17	0.31	0.18
Ventral caudate – Occipital cortex	*r* =	0.18	0.20	0.10
Functional Connectivity ***Hyperactivity/Impulsivity-Related Increase***				
Posterior putamen – Occipital cortex	*r* =	0.12	0.21	0.19
Posterior putamen – Cerebellum	*r* =	0.14	0.19	0.25

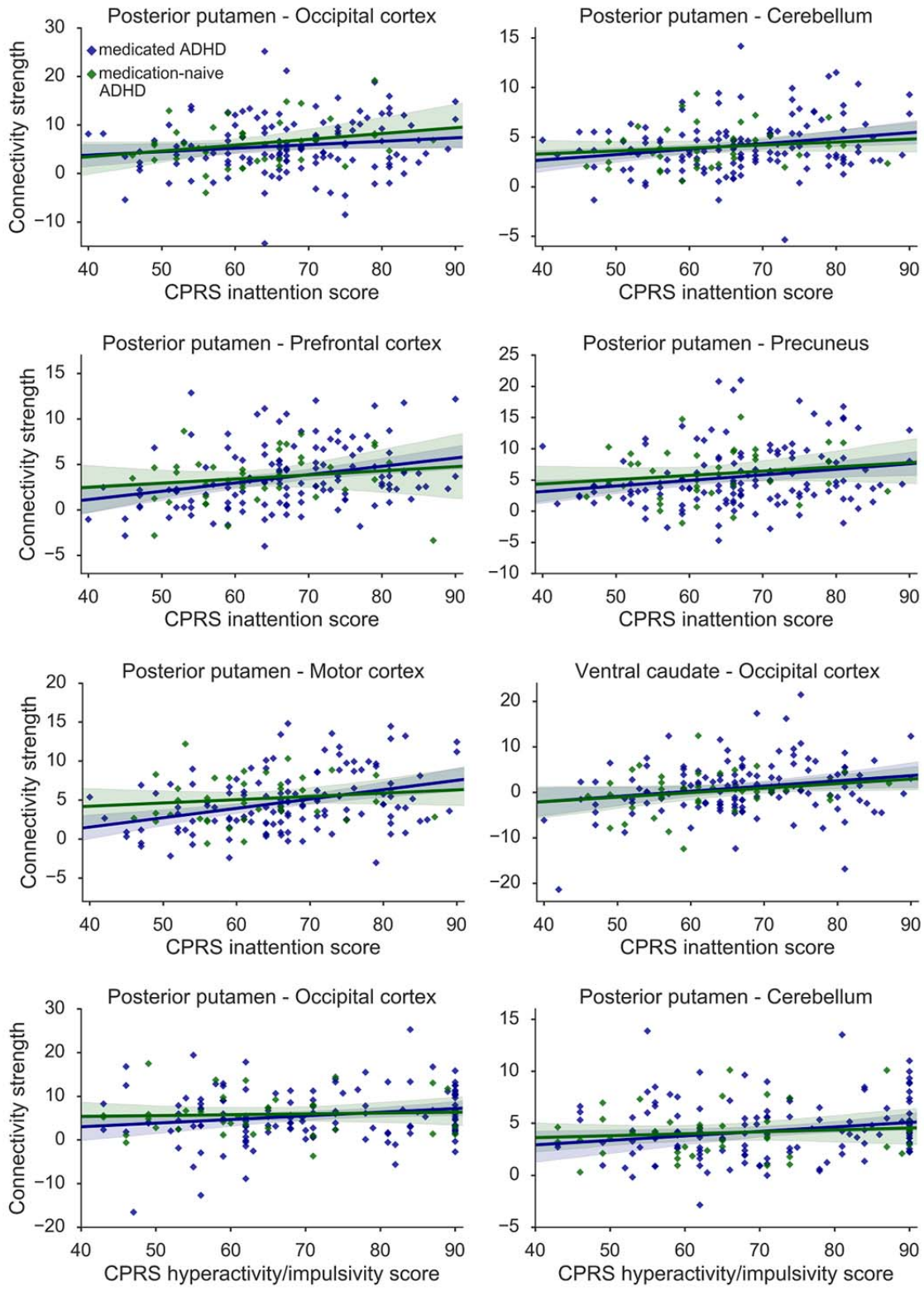

Figure S8. Representation of the observed dimensional relationships between Conners Parent Rating Scale (CPRS) inattention and CPRS hyperactivity/impulsivity scores and functional connectivity of posterior putamen and ventral caudate across medicated ADHD participants (blue) and medication-naive ADHD participants (green).

We ensured that the observed symptom-related increases in functional connectivity in the networks of posterior putamen and ventral caudate were not driven by motion artifacts. To this end, we computed correlations between CPRS inattention scores and CPRS hyperactivity/impulsivity scores and functional connectivity of posterior putamen and ventral caudate with their significant clusters across the entire sample, and included next to covariates for age, sex, scan location, and ODD/CD comorbidity also the root mean squared of the frame-wise displacement as a covariate in our analyses (see Table S6). As can be observed in Table S6, our findings were only very minimally influenced by motion.

Table S6. Correlations and corresponding p-values between Conners Parent Rating Scale (CPRS) inattention scores and posterior putamen-occipital cortex, posterior putamen-cerebellum, posterior putamen-precuneus, posterior putamen-motor cortex, posterior putamen-prefrontal cortex, and ventral caudate-occipital cortex functional connectivity, and between CPRS hyperactivity/impulsivity scores and posterior putamen-occipital cortex and posterior putamen-cerebellum functional connectivity across all subjects without (left; as in original analyses) and with (right) adding the root mean squared of the frame-wise displacement as a covariate (in addition to covariates for age, sex, scan location, oppositional defiant disorder (ODD)/conduct disorder (CD) comorbidity) in the model. These analyses demonstrate that motion artifacts only very minimally influenced our findings. $^{**}p < 0.001$.

Functional Connectivity ***Inattention-Related Increase***		**Corrected for Age, Sex, Scan Location, ODD/CD Comorbidity** (n = 444)	**Corrected for Age, Sex, Scan Location, ODD/CD Comorbidity & the Root Mean Squared of the Frame-Wise Displacement** (n = 444)
Posterior putamen – Occipital cortex	r =	0.26	0.21
	p =	**	**
Posterior putamen – Cerebellum	r =	0.29	0.28
	p =	**	**
Posterior putamen – Precuneus	r =	0.28	0.27
	p =	**	**
Posterior putamen – Motor cortex	r =	0.28	0.27
	p =	**	**
Posterior putamen – Prefrontal cortex	r =	0.24	0.23
	p =	**	**
Ventral caudate – Occipital cortex	r =	0.26	0.26
	p =	**	**
Functional Connectivity ***Hyperactivity/Impulsivity-Related Increase***			
Posterior putamen – Occipital cortex	r =	0.22	0.22
	p =	**	**
Posterior putamen – Cerebellum	r =	0.26	0.25
	p =	**	**

Finally, we correlated connectivity of the identified clusters (obtained using CPRS inattention and CPRS hyperactivity/impulsivity scores) with other ADHD symptom measures. More specifically, we used symptom counts for inattention and hyperactivity/impulsivity obtained from the Schedule for Affective Disorders and Schizophrenia for School-Age Children - Present and Lifetime Version (K-SADS; 12), as well as inattention and hyperactivity/impulsivity scores obtained from either the Conners Adult ADHD Rating Scale (CAARS; 13) for participants ≥ 18 years or the Conners Teacher Rating Scale (CTRS; 14) for participants < 18 years. Table S7 demonstrates that the obtained dimensional effects are consistent across different ADHD symptom measures. Yet, correlations are less strong when using the K-SADS and CAARS/CTRS. This might be explained by lower sensitivity of the K-SADS measure (i.e., K-SADS symptom scores range from 0-9, CPRS symptom scores range from 40-90) and the more heterogeneous CAARS/CTRS symptom measure based on two different scales/informants.

Table S7. Correlations between inattention scores and posterior putamen-occipital cortex, posterior putamen-cerebellum, posterior putamen-precuneus, posterior putamen-motor cortex, posterior putamen-prefrontal cortex, and ventral caudate-occipital cortex functional connectivity, and between hyperactivity/impulsivity scores and posterior putamen-occipital cortex and posterior putamen-cerebellum functional connectivity, calculated using the Conners Parent Rating Scale (CPRS; as in original analyses), Schedule for Affective Disorders and Schizophrenia for School-Age Children - Present and Lifetime Version (K-SADS), and Conners Adult ADHD Rating Scale/Conners Teacher Rating Scale (CAARS)/(CTRS) dependent on the age of the participant. Corrected for effects of age, sex, scan location, and oppositional defiant disorder/conduct disorder comorbidity. *$p < 0.05$, **$p < 0.001$.

Functional Connectivity ***Inattention-Related Increase***		**CPRS** *n* = 444	**K-SADS** *n* = 444	**CAARS/CTRS** *n* = 394
Posterior putamen – Occipital cortex	*r* = *p* =	0.216 **	0.170 **	0.144 **
Posterior putamen – Cerebellum	*r* = *p* =	0.288 **	0.218 **	0.212 **
Posterior putamen – Precuneus	*r* = *p* =	0.283 **	0.190 **	0.143 **
Posterior putamen – Motor cortex	*r* = *p* =	0.279 **	0.208 **	0.170 **
Posterior putamen – Prefrontal cortex	*r* = *p* =	0.238 **	0.236 **	0.159 **
Ventral caudate – Occipital cortex	*r* = *p* =	0.255 **	0.168 **	0.181 **
Functional Connectivity ***Hyperactivity/Impulsivity-Related Increase***				
Posterior putamen – Occipital cortex	*r* = *p* =	0.221 **	0.119 *	0.121 *
Posterior putamen – Cerebellum	*r* = *p* =	0.256 **	0.139 **	0.164 **

Post-hoc Categorical Analysis Using a Non-Bonferroni Corrected Threshold

As we did not observe significant differences between the ADHD and control group in the six striatal functional networks using a Bonferroni corrected threshold of $p < 0.0083$ (i.e., correcting for testing six networks), we additionally investigated whether differences between the ADHD and control group were present in the six networks using a non-Bonferroni corrected threshold set at $p < 0.05$. This analysis revealed an increase in functional connectivity in the network of posterior putamen in the ADHD group. Figure S9 demonstrates increased functional connectivity of posterior putamen with occipital cortex and cerebellum in participants with ADHD. As we observed this trend of increased functional connectivity of posterior putamen in the ADHD compared to the control group, we can thus not state that categorical differences between the ADHD and control group are fully absent. A possible explanation for the absence of significant ADHD versus control group differences might relate to the potential large heterogeneity present in our sample. No differences were found in the other networks.

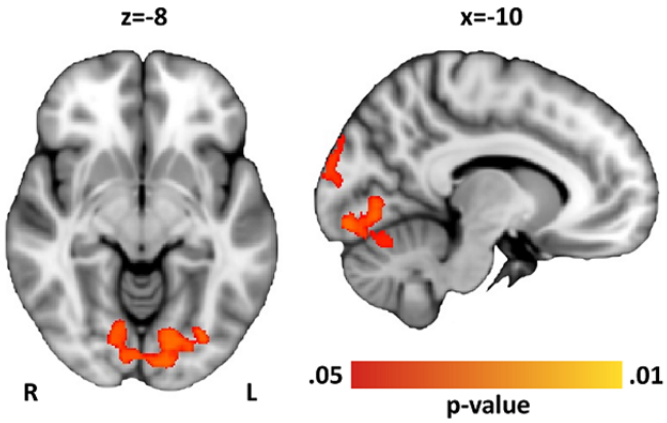

Figure S9. Regions showing higher connectivity with posterior putamen in the ADHD compared to control group using a non-Bonferroni corrected threshold set at $p < 0.05$.

Comparison to ADHD-Related Effects in Networks of Anatomically-Defined Striatal Subregions

To demonstrate the benefit of our functional subdivision over the traditional anatomical subdivision of the striatum when examining striatal connectivity, we also investigated ADHD-related categorical and dimensional effects using putamen, caudate, and NAcc, as anatomically delineated within the Harvard-Oxford subcortical atlas. We did not find significant ADHD versus control group differences in the networks of putamen, caudate, and NAcc. The dimensional analyses did reveal significant inattention-related increases in functional connectivity of putamen with occipital cortex, motor cortex, precuneus, and superior frontal cortex, see Figure S10A. However, these effects appear smaller than the inattention-related increases observed in the network of the functionally defined posterior putamen region (as shown in Figure 3 in the main manuscript and Figure S10B). Furthermore, using the anatomical seed definitions we did not replicate the hyperactivity/impulsivity-related increase in functional connectivity in the network of posterior putamen and the inattention-related increase in functional connectivity in the ventral caudate network. These findings emphasize the added value of using functionally defined, smaller subregions of the striatum to investigate ADHD-related changes in striatal functional connectivity.

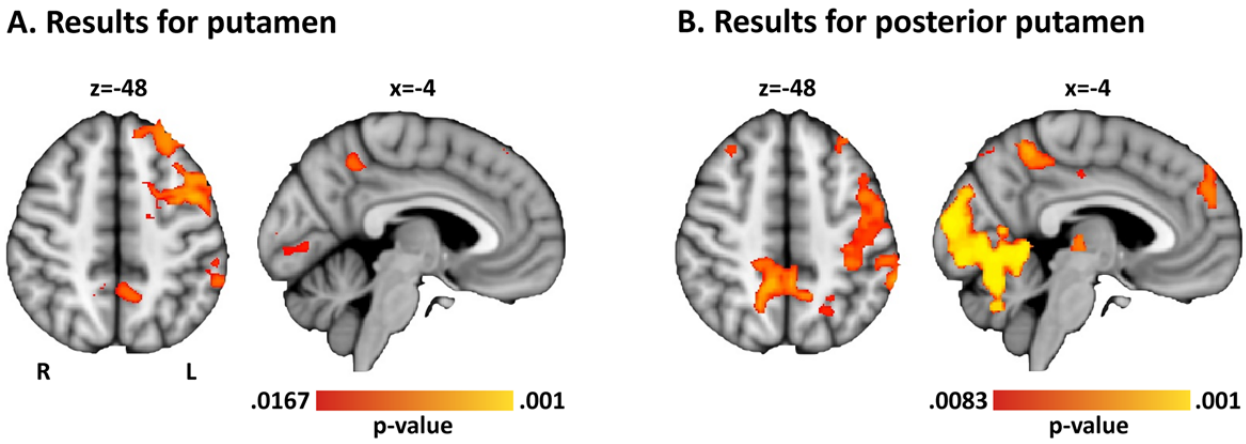

Figure S10. (A) Regions showing an inattention-related increase in functional connectivity with putamen when functional connectivity of the striatum is investigated using putamen, caudate, and NAcc as homogeneous, anatomically defined regions (0.05 / 3 networks = $p < 0.0167$). **(B)** Regions showing an inattention-related increase in functional connectivity with the posterior putamen region defined by the ICP parcellation as described in the main manuscript (see Figures 1 and 3B in the main manuscript; 0.05 / 6 networks = $p < 0.0083$).

Overview of the Measures Used for Motor and Cognitive Performance

Table S8 lists the participant characteristics for the measures of motor performance and cognitive performance that were used in the correlation analyses described in the main manuscript.

Table S8. Motor and cognitive performance characteristics.

	Controls ***n* = 122**		**ADHD** ***n* = 169**		**Subthreshold** ***n* = 64**		**Siblings** ***n* = 89**		**Data Available (% of Sample)**
Measures of Motor Function ***(Mean, SD)***									
DCD-Q total score [a]	71.25	*10.87*	59.56	*12.50*	64.56	*12.33*	67.95	*11.44*	89.9%
Motor timing (RT, ms) [b]	998.9	*87.5*	964.2	*120.3*	982.5	*85.11*	982.0	*106.4*	91.4%
Motor timing (RT variability) [b]	179.2	*59.9*	214.8	*95.6*	190.3	*58.7*	188.0	*61.3*	91.4%
Motor speed (RT, ms) [c]	261.5	*43.5*	269.8	*34.8*	269.2	*37.4*	265.3	*37.9*	90.5%
Motor pursuit [c]	3.08	*0.50*	3.29	*0.74*	3.09	*0.62*	3.20	*0.58*	90.3%
Motor tracking [c]	2.03	*0.69*	2.29	*0.96*	2.04	*0.96*	2.23	*0.99*	90.3%
Measures of Cognitive Function ***(Mean, SD)***									
Visuospatial WM accuracy [d]	0.75	*0.11*	0.71	*0.13*	0.74	*0.10*	0.71	*0.14*	55.0%
SSRT (ms) [e]	260.2	*56.3*	266.5	*55.5*	251.1	*53.0*	264.6	*52.6*	53.8%
Response inhibition errors [e]	2.88	*2.62*	5.42	*5.70*	4.76	*4.50*	3.81	*5.47*	53.8%
WISC/WAIS vocabulary [f]	11.09	*2.82*	8.86	*2.81*	9.70	*2.71*	10.18	*2.89*	99.3%
WISC/WAIS block design [f]	11.11	*2.70*	9.85	*3.12*	10.52	*2.65*	10.48	*3.00*	99.1%

[a] Total motor performance scores obtained from the Developmental Coordination Disorder questionnaire (DCD-Q; 15).

[b] Motor timing (mean reaction time and reaction time variability) based on (16, 17).

[c] Performance on motor speed, motor pursuit (motor control under continuous adaptation), and motor tracking (motor control without continuous adaptation) obtained from the Amsterdam Neuropsychological Task battery (18, 19); performance on motor pursuit is defined as the mean distance (mm) from a continuously moving asterisk that needed to be followed with a cursor; performance on motor tracking is defined as the mean distance (mm) from an imaginary line between an inner and an outer circle that needed to be traced with a cursor.

[d] Accuracy on a visuospatial working memory task (20-22).

[e] Stop Signal Reaction Time (SSRT) and number of errors during a response inhibition task (23, 24).

[f] Normalized scores for vocabulary and block design obtained from the Wechsler Intelligence Scale for Children (WISC; 25) or Wechsler Adults Intelligence Scale (WAIS; 19, 26).

Supplemental References

1. Beckmann CF, Smith SM (2004): Probabilistic independent component analysis for functional magnetic resonance imaging. *IEEE Trans Med Imaging*. 23:137-152.
2. Choi EY, Yeo BT, Buckner RL (2012): The organization of the human striatum estimated by intrinsic functional connectivity. *J Neurophysiol*. 108:2242-2263.
3. Jung WH, Jang JH, Park JW, Kim E, Goo EH, Im OS, et al. (2014): Unravelling the intrinsic functional organization of the human striatum: a parcellation and connectivity study based on resting-state FMRI. *PLoS One*. 9:e106768.
4. Janssen RJ, Jylanki P, Kessels RP, van Gerven MA (2015): Probabilistic model-based functional parcellation reveals a robust, fine-grained subdivision of the striatum. *Neuroimage*. 119:398-405.
5. Yeo BT, Krienen FM, Sepulcre J, Sabuncu MR, Lashkari D, Hollinshead M, et al. (2011): The organization of the human cerebral cortex estimated by intrinsic functional connectivity. *J Neurophysiol*. 106:1125-1165.
6. Di Martino A, Scheres A, Margulies DS, Kelly AM, Uddin LQ, Shehzad Z, et al. (2008): Functional connectivity of human striatum: a resting state FMRI study. *Cereb Cortex*. 18:2735-2747.
7. Jenkinson M, Bannister P, Brady M, Smith S (2002): Improved optimization for the robust and accurate linear registration and motion correction of brain images. *Neuroimage*. 17:825-841.
8. Pruim RH, Mennes M, van Rooij D, Llera A, Buitelaar JK, Beckmann CF (2015): ICA-AROMA: A robust ICA-based strategy for removing motion artifacts from fMRI data. *Neuroimage*. 112:267-277.
9. Pruim RH, Mennes M, Buitelaar JK, Beckmann CF (2015): Evaluation of ICA-AROMA and alternative strategies for motion artifact removal in resting state fMRI. *Neuroimage*. 112:278-287.
10. Greve DN, Fischl B (2009): Accurate and robust brain image alignment using boundary-based registration. *Neuroimage*. 48:63-72.
11. Conners CK, Sitarenios G, Parker JD, Epstein JN (1998): The revised Conners' Parent Rating Scale (CPRS-R): factor structure, reliability, and criterion validity. *J Abnorm Child Psychol*. 26:257-268.
12. Kaufman J, Birmaher B, Brent D, Rao U, Flynn C, Moreci P, et al. (1997): Schedule for Affective Disorders and Schizophrenia for School-Age Children-Present and Lifetime Version (K-SADS-PL): initial reliability and validity data. *J Am Acad Child Adolesc Psychiatry*. 36:980-988.
13. Conners CK, Erhardt D, Sparrow EP (1999): Conners' adult ADHD rating scales (CAARS): technical manual. MHS North Tonawanda.
14. Conners CK, Sitarenios G, Parker JD, Epstein JN (1998): Revision and restandardization of the Conners Teacher Rating Scale (CTRS-R): factor structure, reliability, and criterion validity. *J Abnorm Child Psychol*. 26:279-291.
15. Wilson BN, Kaplan BJ, Crawford SG, Campbell A, Dewey D (2000): Reliability and validity of a parent questionnaire on childhood motor skills. *Am J Occup Ther*. 54:484-493.
16. Rommelse NN, Altink ME, de Sonneville LM, Buschgens CJ, Buitelaar J, Oosterlaan J, et al. (2007): Are motor inhibition and cognitive flexibility dead ends in ADHD? *J Abnorm Child Psychol*. 35:957-967.
17. Thissen AJ, Luman M, Hartman C, Hoekstra P, van Lieshout M, Franke B, et al. (2014): Attention-deficit/hyperactivity disorder (ADHD) and motor timing in adolescents and their parents: familial characteristics of reaction time variability vary with age. *J Am Acad Child Adolesc Psychiatry*. 53:1010-1019 e1014.

18. De Sonneville L (1999): Amsterdam Neuropsychological Tasks: A computer-aided assessment program. *Computers in psychology*. 6:187-203.
19. Thissen AJ, Rommelse NN, Altink ME, Oosterlaan J, Buitelaar JK (2014): Parent-of-origin effects in ADHD: distinct influences of paternal and maternal ADHD on neuropsychological functioning in offspring. *J Atten Disord*. 18:521-531.
20. Klingberg T, Forssberg H, Westerberg H (2002): Training of working memory in children with ADHD. *J Clin Exp Neuropsychol*. 24:781-791.
21. McNab F, Leroux G, Strand F, Thorell L, Bergman S, Klingberg T (2008): Common and unique components of inhibition and working memory: an fMRI, within-subjects investigation. *Neuropsychologia*. 46:2668-2682.
22. van Ewijk H, Heslenfeld DJ, Luman M, Rommelse NN, Hartman CA, Hoekstra P, et al. (2014): Visuospatial working memory in ADHD patients, unaffected siblings, and healthy controls. *J Atten Disord*. 18:369-378.
23. Logan GD, Cowan WB, Davis KA (1984): On the ability to inhibit simple and choice reaction time responses: a model and a method. *J Exp Psychol Hum Percept Perform*. 10:276-291.
24. van Rooij D, Hoekstra PJ, Mennes M, von Rhein D, Thissen AJ, Heslenfeld D, et al. (2015): Distinguishing Adolescents With ADHD From Their Unaffected Siblings and Healthy Comparison Subjects by Neural Activation Patterns During Response Inhibition. *Am J Psychiatry*. 172:674-683.
25. Wechsler D (2002): WISC-III Handleiding. The Psychological Corporation, London.
26. Wechsler D (2000): WAIS-III Nederlandstalige bewerking. Technische handleiding. The Psychological Corporation, London.